Article

Standard Electrochemical Behavior of High-Quality, Boron-Doped Polycrystalline Diamond Thin-Film Electrodes

Michael C. Granger, Malgorzata Witek, Jishou Xu, Jian Wang, Mateusz Hupert, Amy Hanks, Miles D. Koppang, James E. Butler, Guy Lucazeau, Michel Mermoux, Jerzy W. Strojek, and Greg M. Swain

Anal. Chem., **2000**, 72 (16), 3793-3804• DOI: 10.1021/ac0000675 • Publication Date (Web): 21 July 2000

Anal. Chem. **2000,** *72,* 3793−3804

Standard Electrochemical Behavior of High-Quality, Boron-Doped Polycrystalline Diamond Thin-Film Electrodes

Michael C. Granger,[†] Malgorzata Witek,[†] Jishou Xu,[†] Jian Wang,[†] Mateusz Hupert,[†] Amy Hanks,[†] Miles D. Koppang,[‡] James E. Butler,[§] Guy Lucazeau,[∥] Michel Mermoux,[∥] Jerzy W. Strojek,[⊥] and Greg M. Swain*,[†]

Department of Chemistry and Biochemistry, Utah State University, Logan, Utah 84322-0300, Department of Chemistry, University of South Dakota, Vermillion, South Dakota 57069, Chemistry Division, Naval Research Laboratory, Code 6174, Washington, D.C. 20375-5000, Laboratoire d'Electrochimie et de Physicochimie des Matériaux et Interfaces, UMR 5631 INPG−CNRS, associée à l'UJF, Domaine Universitaire, BP 75, 38402 Saint Martin d'Hères, Cedex, France, and Faculty of Chemistry, Silesian Technical University, Gliwice 44-100, Poland

Standard electrochemical data for high-quality, boron-doped diamond thin-film electrodes are presented. Films from two different sources were compared (NRL and USU) and both were highly conductive, hydrogen-terminated, and polycrystalline. The films are acid washed and hydrogen plasma treated prior to use to remove nondiamond carbon impurity phases and to hydrogen terminate the surface. The boron-doping level of the NRL film was estimated to be in the mid 10^{19} B/cm^3 range, and the boron-doping level of the USU films was $\sim 5 \times 10^{20}$ B/cm^{-3} based on boron nuclear reaction analysis. The electrochemical response was evaluated using $Fe(CN)_6^{3-/4-}$, $Ru(NH_3)_6^{3+/2+}$, $IrCl_6^{2-/3-}$, methyl viologen, dopamine, ascorbic acid, $Fe^{3+/2+}$, and chlorpromazine. Comparisons are made between the apparent heterogeneous electron-transfer rate constants, k^o_{app}, observed at these high-quality diamond films and the rate constants reported in the literature for freshly activated glassy carbon. $Ru(NH_3)_6^{3+/2+}$, $IrCl_6^{2-/3-}$, methyl viologen, and chlorpromazine all involve electron transfer that is insensitive to the diamond surface microstructure and chemistry with k^o_{app} in the $10^{-2}-10^{-1}$ cm/s range. The rate constants are mainly influenced by the electronic properites of the films. $Fe(CN)_6^{3-/4-}$ undergoes electron transfer that is extremely sensitive to the surface chemistry with k^o_{app} in the range of $10^{-2}-10^{-1}$ cm/s at the hydrogen-terminated surface. An oxygen surface termination severely inhibits the rate of electron transfer. $Fe^{3+/2+}$ undergoes slow electron transfer at the hydrogen-terminated surface with k^o_{app} near 10^{-5} cm/s. The rate of electron transfer at sp^2 carbon electrodes is known to be mediated by surface carbonyl functionalities; however, this inner-sphere, catalytic pathway is absent on diamond due to the hydrogen termination. Dopamine, like other catechol and catecholamines, undergoes sluggish electron transfer with k^o_{app} between 10^{-4} and 10^{-5} cm/s. Converting the surface to an oxygen termination has little effect on k^o_{app}. The slow kinetics may be related to weak adsorption of these analytes on the diamond surface. Ascorbic acid oxidation is very sensitive to the surface termination with the most negative E_p^{ox} observed at the hydrogen-terminated surface. An oxygen surface termination shifts E_p^{ox} positive by some 250 mV or more. An interfacial energy diagram is proposed to explain the electron transfer whereby the midgap density of states results primarily from the boron doping level and the lattice hydrogen. The films were additionally characterized by scanning electron microscopy and micro-Raman imaging spectroscopy. The cyclic voltammetric and kinetic data presented can serve as a benchmark for research groups evaluating the electrochemical properties of semimetallic (i.e., conductive), hydrogen-terminated, polycrystalline diamond.

Boron-doped diamond thin-film electrodes possess important properties, particularly for electroanalysis.[1−9] In recent years, several groups have made progress understanding the factors that influence the electrochemical response of these materials including those of Fujishima (Japan), Pleskov (Russia), Tenne (Israel), Angus and Miller (U.S.A.), and Compton (England). While interesting and, in some cases, unique behavior of diamond

[†] Utah State University.
[‡] University of South Dakota.
[§] Naval Research Laboratory.
[∥] Domaine Universitaire.
[⊥] Silesian Technical University.

(1) Xu, J.; Granger, M. C.; Chen, Q.; Lister, T. E.; Strojek, J. W.; Swain, G. M. *Anal. Chem*., **1997**, *69*, 591A.
(2) Swain, G. M.; Anderson, A.; Angus, J. C. *MRS Bull.* **1998**, *23*, 56.
(3) Tenne, R.; Lévy-Clément, C. *Isr. J. Chem*., **1998**, *38*, 57.
(4) Pleskov, Y. V. *Russ. Chem. Rev*. **1999**, *68*, 381.
(5) Alehashem, S.; Chamber, F.; Strojek, J. W.; Swain, G. M.; Ramesham, R. *Anal. Chem*. **1995**, *67*, 2812.
(6) Jolley, S.; Koppang, M.; Jackson, T.; Swain, G. M. *Anal. Chem*. **1997**, *69*, 4041.
(7) Xu, J.; Swain, G. M. *Anal. Chem*. **1998**, *70*, 1502.
(8) Koppang, M. D.; Witek, M.; Blau, J.; Swain, G. M. *Anal. Chem*. **1999**, *71*, 1188.
(9) Rao, T. N.; Yagi, I.; Miwa, T.; Tryk, D. A.; Fujishima, A. *Anal. Chem*. **1999**, *71*, 2506.

10.1021/ac0000675 CCC: $19.00
Published on Web 07/21/2000

electrodes has been demonstrated,[1−4] there can be significant variability in the response, as reported in results from different laboratories. In our opinion, this variability is due to two factors: (i) the solution conditions, surface cleanliness, redox analyte selected to probe the reactivity and electrolyte composition and (ii) film quality issues. Several factors can influence the electrochemical response of polycrystalline diamond films: (i) nondiamond carbon impurity phases, (ii) the surface termination (H vs O), (iii) the dopant type, level, and distribution, (iv) grain boundaries and other morphological defects, and (v) the primary crystallographic orientation. The extent to which one or more of these factors influences the response will depend on the charge-transfer mechanism of the particular redox analyte.[10−15] *At present, there is no standard diamond electrode material to compare results against*. Since diamond is a new electrode material with only a brief history of use, it is vital that researchers pay careful attention to the physicochemical properties of the films, the solution composition (e.g., pH and electrolyte), and the redox mechanism for the particular analyte used to probe the activity when evaluating performance.

In this article, we present cyclic voltammetric data for several redox analytes at high-quality, boron-doped, polycrystalline diamond thin films from two different sources. *By high quality we mean clean, electrically conducting, hydrogen-terminated, polycrystalline films with negligible nondiamond carbon impurity phases at the surface and low levels of secondary nuclei formed on the primary diamond microcrystallites.* The boron-doping level of the NRL film was estimated to be in the low 10^{19} B/cm^3 range, while the doping level of the USU films was $\sim 5 \times 10^{20}$ B/cm^3. The film surfaces were cleaned of nondiamond carbon impurity phases by a two-step acid washing procedure and hydrogen-terminated by a subsequent hydrogen plasma treatment. Several aqueous-based redox systems were used to probe the films'electrochemical response. There were two reasons for selecting these redox systems: (i) the known sensitivity or insensitivity of each to the electronic properties, surface microstructure, and surface chemistry of sp^2 and sp^3 carbon electrodes and (ii) the wide range of formal potentials ($\sim$+0.9 to −1.0 V vs SCE). The electrochemical response of a recognized high-quality polycrystalline film produced by the NRL group is compared with the response of our high-quality films. It is our opinion that these data can serve as a benchmark for research groups evaluating the electrochemical properties of polycrystalline, hydrogen-terminated, boron-doped diamond electrodes. Scanning electron microscopy was used to examine the film morphology, and micro-Raman imaging spectroscopy was employed to probe the film microstructure, in addition to the electrochemical measurements.

EXPERIMENTAL SECTION

Diamond Thin-Film Deposition. Diamond films used were deposited by the USU group using microwave-assisted chemical vapor deposition (CVD) (1.5 kW, 2.54 GHz, Astex, Lowell, MA). The films were grown on conducting p-Si (100) substrates. The substrates (0.1 cm thick × 1 cm^2 in area) were first pretreated by solvent washing in toluene, methylene chloride, acetone, 2-propanol, and methanol. The substrates were then etched in concentrated hydrofluoric acid for 60 s after air-drying. After rinsing with ultrapure water and drying, the substrates were sonicated in a diamond powder/acetone slurry (0.1-μm diameter, GE Superabrasives, Worthington, OH) for 20 min. The substrates were then rinsed with clean acetone and placed in the CVD reactor. The sonication "seeds" the surface with diamond particles ($>10^8$ particles/cm^2, as estimated by atomic force microscopy) that serve as nucleation centers during film growth. High-quality, polycrystalline diamond thin films were deposited using a methane/hydrogen (C/H) mixture with a *volumetric ratio* of 0.33% at a total flow of 200 sccm, a forward power of 1000 W, a system pressure of 40 Torr, a substrate temperature of $\sim$850 °C (as measured by a disappearing filament optical pyrometer), and a growth time of $\sim$20 h. The C/H ratio refers to the composition of the source gases flowing into the reactor, not the final elemental ratio in the films. Ultrahigh purity (99.999%) methane and hydrogen were used as the source gases. The films were doped using solid-state sources: a boron diffusion source (GS-126, BoronPlus, Techniglas, Inc., Perrysburg, OH) and a small piece of boron nitride (Goodfellow, Ltd., Cambridge, England). The substrates were placed on top of the diffusion source and adjacent to the piece of boron nitride in the center of the 3-in.-diameter molybdenum substrate stage. The film thickness was $\sim$5 μm based on growth rate calculations, and the boron dopant concentration was $\sim 5 \times 10^{20}$ B/cm^3 (3000 ppm or 0.3% B/C) based on boron nuclear reaction analysis measurements (Center for Materials Characterization, Case Western Reserve University). Film resistivity measurements using a tungsten four-point probe (with the diamond attached to the conducting Si substrate) yielded values between 0.1 and 0.01 Ω·cm.

The substrates were heated to the growth temperature in a hydrogen plasma for 10−15 min prior to introducing the methane. The plasma was formed with a hydrogen flow of 200 sccm, a system pressure of 40 Torr, and a forward power of 1000 W. After deposition, the methane flow was stopped, and the films remained exposed to the hydrogen plasma for an additional 10 min at 40 Torr and 1000 W. Further hydrogen annealing was continued in the following manner: 10 min at 800 W and 30 Torr, 10 min at 600 W and 20 Torr, 10 min at 400 W and 10 Torr, and 5 min at 200 W and 10 Torr. This procedure cools the samples to $\sim$300 °C in the presence of atomic hydrogen. Postgrowth annealing in atomic hydrogen is essential for etching away adventitious nondiamond impurities, minimizing dangling bonds, and ensuring full hydrogen termination. The plasma was then extinguished and the films further cooled to room temperature under a flow of hydrogen.

Several *free-standing* ($\sim$300 μm), high-quality, polycrystalline films were provided by the group at the Naval Research Laboratory. These films (NRL-148 and 143) were grown on Si substrates by microwave-assisted CVD using a C/H ratio of $\sim$0.8% with a total flow of 130 sccm, a forward power of $\sim$4 kW, a system pressure of 117 Torr, a substrate temperature of 810 °C (as measured with an optical pyrometer), and a 0.4 sccm flow of 0.1% $^{10}B_2H_6$ in hydrogen for boron doping. After growth, the samples were cooled to $\sim$250 °C in the presence of atomic hydrogen before

(10) Kneten, K. R.; McCreery, R. L. *Anal. Chem.* **1992**, *64*, 2518.
(11) Chen, P.; Fryling, M. A.; McCreery, R. L. *Anal. Chem.* **1995**, *67*, 3115.
(12) Chen, P.; McCreery, R. L. *Anal. Chem.* **1996**, *68*, 3958.
(13) Ranganathan, S.; Kuo, T.-C.; McCreery, R. L. *Anal. Chem.* **1999**, *71*, 3574.
(14) Yang, H.-H.; McCreery, R. L. *Anal. Chem.* **1999**, *71*, 4081.
(15) Hunt-DuVall, S.; McCreery, R. L. *Anal. Chem.* **1999**, *71*, 4594.

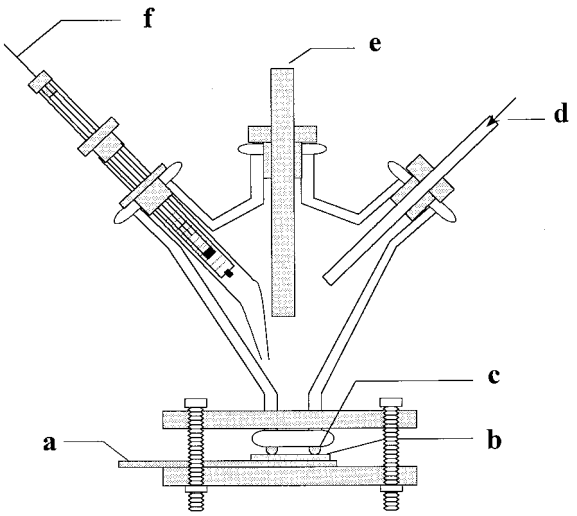

Figure 1. Diagram of the single-compartment, glass electrochemical cell used. (a) Cu or Al metal current collecting plate, (b) diamond film electrode, (c) Viton O-ring seal, (d) input for nitrogen purge gas, (e) carbon rod or Pt counter electrode, and (f) reference electrode inside a glass capillary tube with a cracked tip.

extinguishing the plasma. The actual boron-doping level in these films was not measured, but the conductive films had an in-plane resistivity near 0.01 Ω·cm, similar to the USU films.

Film Cleaning. The films were pretreated by a two-part acid washing procedure to remove nondiamond carbon impurity phases and to clean the surface. This was done in a small 50-mL Pyrex beaker with a glass lid to help trap and condense the vapors. First, they were gently refluxed in aqua regia (3 HCl/1 HNO_3) for 30 min to remove metallic impurities. The films were then rinsed in distilled H_2O and dried. Second, they were refluxed in a concentrated $H_2SO_4/HNO_3/NaNO_3$ solution to remove nondiamond carbon deposits from the surface. The acid-washed films were then hydrogen plasma treated at 800 °C, 20 or 30 Torr, and 1000 W for 30 min to remove surface oxygen and rehydrogenate the surface. After plasma treatment, the samples were slowly cooled in the presence of atomic hydrogen, as described above. We have found that this treatment is also effective at activating diamond electrodes with extensive past histories. The acid washing introduces oxygen functionalities on the surface. Typical XPS atomic O/C ratios after acid washing were near 0.15, decreasing to 0.02 or less after rehydrogenation in the hydrogen plasma.

Electrochemical Measurements. The electrochemical measurements were performed in a single compartment glass cell using either an Omni-90 analog or a CYSY-2000 digital potentiostat (Cypress Systems, Inc., Lawrence, KS). Figure 1 shows a diagram of the cell. A commercial saturated calomel electrode (SCE) was used as the reference and a large-area carbon rod served as the counter electrode. The diamond film electrodes were pressed against the bottom of the glass cell with the fluid being contained by a Viton O-ring. The exposed geometric area was 0.2 cm^2, and all currents are normalized to this area. The large-area counter electrode was placed parallel to the working electrode. The reference electrode was positioned near the working electrode using a cracked glass capillary. Electrical connection was made to the diamond in one of three ways with each method generally providing similar results: (i) scratching the backside of the Si substrate with a diamond scribe and then coating the area with graphite from a pencil before contacting the Al current collecting backplate, (ii) same as above but coating the area with Ag paste, or (iii) same as above but running a bead of Ag paste from the top edge of the diamond film to the backside of the Si substrate or the diamond film in the case of the free-standing materials. The Al plate was polished clean prior to contact. Care must be taken to avoid solution leakage, which can cause formation of salt deposits on the backside of the Si substrate and prevent good electrical contact with the current collecting plate. More recently, we have been using an In/Ga eutectic to make ohmic contact to the backside of the scratched Si substrate. All measurements were made at room temperature (23 ± 2 °C) in solutions deoxygenated by nitrogen purge gas. The mounted diamond film working electrodes were rinsed with ultrapure water (>17 MΩ·cm, Barnstead Nanopure), soaked for 20 min in distilled 2-propanol, and rinsed with ultrapure water again prior to use. 2-Propanol can be an effective cleaning agent for sp^2 carbon electrodes.[13] A three-step cleaning procedure was used for all glassware: washing in a KOH/methanol bath, washing in a liquid detergent/water bath (Alconox, Inc.), and rinsing with ultrapure water.

Film Characterization. The scanning electron microscopy was performed using a Hitachi 4000S microscope. The images were constructed with both backscattered and secondary electrons. The instrument is housed in the Electron Microscopy facility at USU.

The macro-Raman spectroscopy (USU) was performed in a 180° backscattered collection mode using an Explorer I (Instruments SA) system consisting of an air-cooled 100-mW Ar^+ laser (514.5 nm, Omnichrome), a 1.25-m spectrometer (f/11, 1800 grooves/mm holographic grating), a 1428E MicraMate confocal microscope assembly (aperature of 200 μm), and a Spectrum One 2000 × 800 CCD detector. Spectra were collected with an incident power density of ~50 kW/cm^2 (10 mW at the sample and 5-μm-diameter spot size). The spectrometer was calibrated using the 521-cm^{-1} one-phonon line from a piece of single-crystal Si, or the 1332.5-cm^{-1} one-phonon line from a synthetic IIb diamond chip (Harris Diamond). The micro-Raman imaging spectroscopy (France) was performed using a Dilor XY confocal spectrometer equipped with a CCD array detector, using the 514.5-nm line of an Ar ion laser.[16,17] The laser power was held constant throughout the experiments with generally 20 mW incident on the samples. A confocal aperature of 600 μm was used.

Chemicals. All chemicals were reagent grade quality or better and used without additional purification. Solutions (1 mM) of potassium ferrocyanide (Aldrich), hexaminеruthenium(III) chloride (Aldrich), potassium hexachloroiridate (IV) (Aldrich), methyl viologen dichloride hydrate (Aldrich), 2-chloro-10-(3-dimethylaminopropyl)phenothiazine (chlorpromazine, CPZ, Sigma), ferric sulfate (Matheson Coleman and Bell), ascorbic acid (Aldrich), dopamine (Aldrich), 4-methylcatechol (Aldrich), and 4-*tert*-butylcatechol (Aldrich) were prepared. The supporting electrolyte for all solutions was either 1 M KCl (Fisher Scientific) or 1 M $HClO_4$ (99.999%, Aldrich). All solutions were prepared with ultrapure water from a Barnstead E-Pure purification system (18 MΩ·cm).

(16) Haouni, A.; Mermoux, M.; Marcus, B.; Abello, L.; Lucazeau, G. *Diamond Relat. Mater.* **1999**, *8*, 657.
(17) Wang, J.; Swain, G. M.; Mermoux, M.; Lucazeau, G.; Zak, J.; Strojek, J. W. *New Diamond Frontier Carbon Technol.* **1999**, *9*, 317.

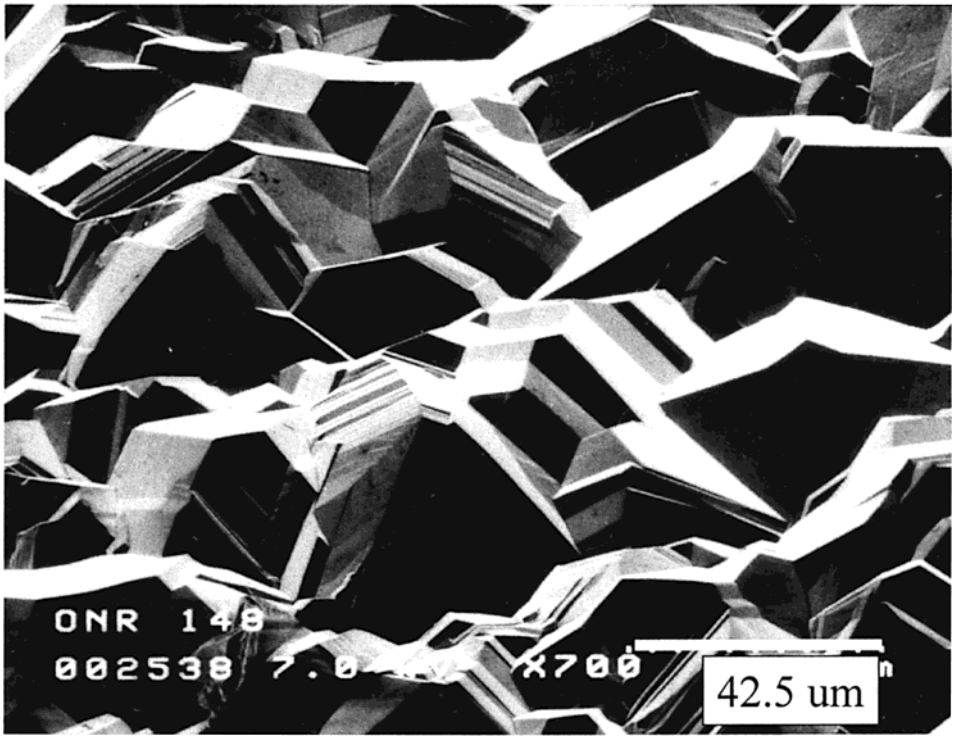

Figure 2. Scanning electron micrograph of a high-quality diamond film from NRL (No. 148).

RESULTS AND DISCUSSION

Morphology and Microstructure. Figure 2 shows a scanning electron micrograph of a free-standing, polycrystalline NRL film (No. 148). The film is continuous over the surface and the morphology displays cubooctahedral habits—microcrystallites of cubic (100) and octahedral (111) crystallographic orientation. Many of the microcrystallites have a nominal diameter of ~40 μm. The grain boundaries and facet surfaces, for the most part, are void of smaller diamond growths (i.e., secondary nuclei). The {111} faces are the preferred growth planes. Comparatively, the USU diamond films deposited on Si substrates have a similar continuous, well-faceted, and low secondary growth morphology, but with a smaller nominal crystallite size of 1−4 μm.[1,24] The smaller nominal crystallite size leads to a higher fraction of exposed grain boundaries. No gross changes in the morphology of either film were detected after acid washing and rehydrogenation.

Figure 3A−E shows micro-Raman spectral data for NRL (No. 143) and USU films. The data presented are the average of 2500 spectra obtained over a 25 × 25 μm^2 area with a point spacing of ~0.5 μm. Figure 3A shows the average Raman spectra from two different regions on the NRL film. The spectra are characteristic of high-quality diamond (narrow line width and low background signal). A very intense one-phonon diamond line is observed near 1332 cm^{-1} with a line width of 2−3 cm^{-1}. This compares favorably

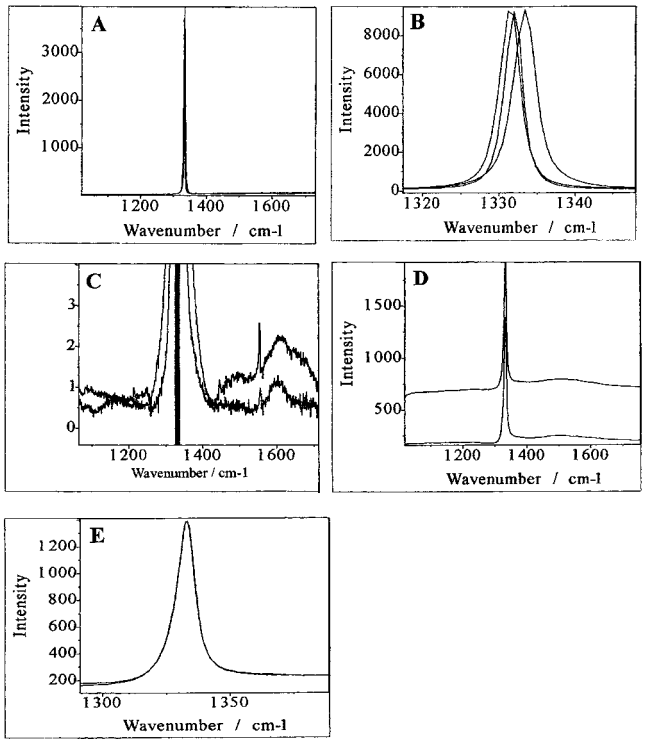

Figure 3. Micro-Raman spectra from a high-quality NRL diamond film (No. 143) (A−C) and from a high-quality USU film (D, E). (A) Spectra from two different regions on the film surface. (B) One-phonon diamond line from three different regions on the film surface. (C) Enlargement of the spectra shown in (A) revealing the scattering by nondiamond carbon impurity phases. (D) Spectra from two different regions on the film surface. (E) One-phonon diamond line from two different regions on the film surface.

(18) Robins, L. H.; Farabaugh, E. N.; Feldman, A. *J. Mater. Res.* **1990**, *5*, 2456.
(19) Ager, J. W., III; Walukiewicz, W.; McCluskey, M.; Plano, M. A.; Landstrass, M. I. *Appl. Phys. Lett.* **1995**, *66*, 616.
(20) Gonon, P.; Gheeraert, E.; Deneuville, A.; Fontaine, F.; Abello, L.; Lucazeau, G. J. *Appl. Phys.* **1995**, *78*, 7059.
(21) Knight, D. S.; White, W. B. *J. Mater. Res.* **1989**, *4*, 385.
(22) Marcus, B.; Fayette, L.; Mermoux, M.; Abello. L.; Lucazeau, G. *J. Appl. Phys.* **1994**, *76*, 3463.
(23) Yarbrough, W. A.; Messier, R. *Science* **1990**, *247*, 688.
(24) Granger, M. C.; Xu, J.; Strojek, J. W.; Swain, G. M. *Anal. Chim. Acta* **1999**, *397*, 145.

with the 2−3-cm^{-1} width observed for the one-phonon line of a single-crystal diamond standard. The line width is a qualitative measure of the crystalline quality of the film. The more defects there are in the probed area, the shorter the phonon lifetime and the broader the line width. The average line position is 1331.3 cm^{-1}, compared to the 1331.9 cm^{-1} for a high-pressure, high-temperature reference diamond. The line position is relatively constant varying only from 1331.5 to 1335.5 cm^{-1} over the probed area, as seen in Figure 3B. The band shift to higher wavenumbers is indicative of a slight compressive stress.[16−18] The diamond lines are very symmetric consistent with a moderate boron-doping level of $\sim 10^{19}$ B/cm^3.[19,20,24] The diamond line position, width, and other spectral features, are highly sensitive to the doping level.[17,19,20,24] The spectra have a very low background luminescence signal and no apparent scattering by nondiamond carbon impurity phases between 1500 and 1600 cm^{-1}. However, it is possible to detect extremely low levels of these impurity phases if the intensity scale is expanded, as shown in Figure 3C. The spectrum from one region shows a weak peak at ~1590 cm^{-1} while the spectrum from another region shows slightly more intense peaks at 1500 and 1590 cm^{-1}. These data suggest that there is some minor variability in the distribution of nondiamond carbon impurity phases spatially within the film, but qualitatively, the levels are extremely low as assessed by comparing the 1332−1590-cm^{-1} peak intensity ratios. The low level of these impurities is further evidenced if the Raman scattering cross section coefficients are considered as the cross section for graphite (assumed to be the nondiamond carbon impurity type) is 50 times larger than for diamond using the 514.5-nm excitation light.[21] The 1590-cm^{-1} peak suggests that some of the nondiamond carbon phases have microstructural order (i.e., graphite-like) while the 1500-cm^{-1} peak is more characteristic of amorphous carbon (i.e., a mixture of sp^2 and sp^3 bonding).[22,23] The narrow line at 1556 cm^{-1} is due to the O_2 stretching mode. In summary, there were only minor variations in the spectral features over the 25 × 25 μm^2 imaged area, indicative of a highly uniform diamond film microstructure.

Panels D and E of Figure 3 show average micro-Raman spectra from two regions on a USU film. Again, the data shown are the average of 2500 spectra obtained from a 25 × 25 μm^2 region. The spectra are nearly identical with the only difference being the level of the background luminescence. The one-phonon diamond line is centered near 1332.5 cm^{-1}, and the line width is ~6 cm^{-1}. The line width varied from 5 to 10 cm^{-1} over the imaged area. The higher luminescence and the larger line width for the USU film, compared to the NRL film, is due to the smaller grain size of the former, hence a higher defect density within the probed volume. A measurement at the NRL film is probing one grain while multiple grains and intercrystalline grain boundaries are probed at the USU film. The line position varied narrowly over a range from 1331 to 1334 cm^{-1}. There is also a weak peak centered near 1500 cm^{-1} attributable to nondiamond carbon impurities incorporated into the near-surface region of the film. The diamond line is asymmetric with an upward shift in intensity on the high wavenumber side of the peak. This shift is attributed to a Fano-type interference between scattering by the zone-center optical phonon and scattering by the electronic continuum associated with the formation of a boron dopant impurity band above 10^{19} B/cm^3 whose energy overlaps that of the phonon.[19,20,24] In summary, both films are diamond in character with low levels of nondiamond carbon impurity phases. These impurities exist in the near-surface region and not on the surface as the acid washing and rehydrogenation are expected to completely remove these phases. The microstructure and optical properties of both films are fairly uniform across the surface. Again, the smaller nominal grain size of the USU film leads to a higher fraction of exposed grain boundary, hence a larger diamond line width and a slightly higher background luminescence, compared to the NRL film.

Electrochemical Characterization. Background cyclic voltammetric $i-E$ curves are useful for examining the diamond film quality because the electrochemical response is *highly sensitive* to physicochemical properties of the *surface. The magnitude of the background current, the working potential window, and the voltammetric features present within the working potential window are all sensitive to the presence of nondiamond (amorphous or graphitic) carbon impurities.*[1−3,17,24,26] Depending on the deposition conditions and the cool-down protocol postdeposition, nondiamond carbon impurities can exist (i) as a reconstructed layer on the surface, (ii) as an extended defect within the diamond lattice, and/or (iii) in the intercrystalline grain boundaries. Typically, high-quality films have a flat and featureless voltammetric response in the potential range from −500 to +1000 mV vs SCE (acidic or neutral pH), with a background current density (per geometric area) ~10 times lower than polished glassy carbon.[1,2,17,24,25] Surface nondiamond carbon impurities are more reactive (e.g., intercalation, surface oxidation, and gasification to CO and CO_2) than diamond is, and this increased reactivity causes a larger background current.[2,24,26] These impurities also likely affect the electronic properties of the film by increasing the potential-dependent density of electronic states in the midgap region. The increased surface charge density is manifested in a larger double-layer charging current.

Figure 4A shows background cyclic voltammetric $i-E$ curves in 0.1 M H_2SO_4 for NRL (No. 148) and USU films. The films were acid washed and rehydrogenated so surface nondiamond carbon impurity phases are not influencing the response. The background current for the NRL film is low and featureless between −2000 and 1600 mV. There is no evidence for surface redox processes; therefore, the film appears to be ideally polarizable in this potential region. A similarly low and featureless background current is observed for the USU film between −800 and 1800 mV. The background currents for both electrodes are a factor of ~10 lower than freshly polished glassy carbon (per geometric area). No change in the shape of the traces was observed during multiple cycles suggestive of a very stable surface structure. The working potential window (±500 $\mu A/cm^2$ geometric) for these two films is 4.4 and 3.4 V, respectively. The true current density is actually lower than this due to the estimated roughness factor of 2−5. The window for the NRL film is the widest we have ever observed for any conductive microcrystalline diamond film, particularly at negative potentials. This includes films from our laboratory and other laboratories around the world (NIRIM, Japan, Kobe Steel Ltd., Japan, etc.). Clearly, the overpotential for hydrogen evolution at this particular NRL film is 1 V larger than at the USU film. The 3.4-V window for the USU film is within the range of 3−4 V

(25) Xu, J.; Chen, Q.; Swain, G. M. *Anal. Chem.* **1998**, *70*, 3146.
(26) Martin, H. B.; Argoitia, A.; Landau, U.; Anderson, A. B.; Angus, J. C. *J. Electrochem. Soc.* **1996**, *143*, L133.

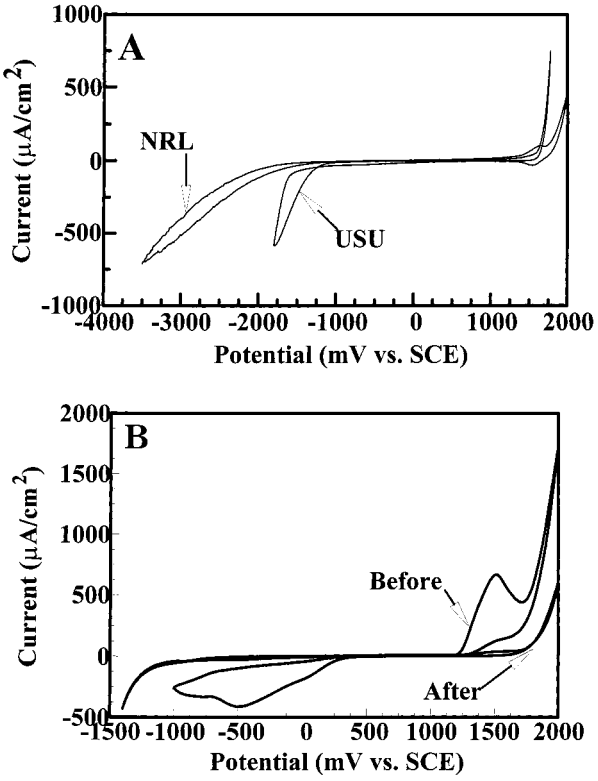

Figure 4. (A) Cyclic voltammetric $i-E$ curves for high-quality NRL (No. 148) and USU films in 0.1 M H_2SO_4. Scan rate, 0.1 V/s. (B) Cyclic voltammetric $i-E$ curves for a lower quality USU film in 0.1 M H_2SO_4 before and after acid washing and rehydrogenation. Scan rate, 0.1 V/s.

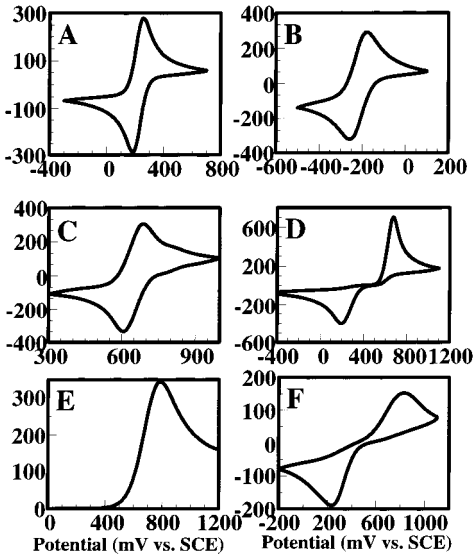

Figure 5. Cyclic voltammetric $i-E$ curves for (A) 1 mM $Fe(CN)_6^{3-/4-}$ in 1 M KCl, (B) 1 mM $Ru(NH_3)_6^{3+/2+}$ in 1 M KCl, (C) 1 mM $IrCl_6^{2-/3-}$ + 1 M KCl, (D) 1 mM dopamine in 1 M $HClO_4$, (E) 1 mM ascorbic acid in 1 M $HClO_4$, and (F) 1 mM $Fe^{3+/2+}$ in 1 M $HClO_4$. Scan rate, 0.1 V/s. *Y*-axis on all voltammograms is current density (μA/cm^2).

typically observed for most boron-doped, polycrystalline diamond films.[1−3,17,24,26] We suppose the larger potential window for the NRL film is due, in part, to the lower fraction of exposed grain boundaries. It could also be due to the slightly lower boron-doping level, which would reduce the density of electronic states at negative potentials. These two examples would appear to suggest that there is a considerable variance in the behavior of diamond films from source to source; however, this is not the case. The uncharacteristically large working potential window for this particular NRL film is the exception rather than the rule for conductive diamond.

Figure 4B shows an extreme example of how acid washing and rehydrogenation affects the background voltammetric response of a low-quality diamond film (i.e., significant level of nondiamond carbon impurities). The cyclic voltammetric $i-E$ curve in 0.1 M H_2SO_4 for the film prior to treatment shows an anodic peak on the forward sweep at 1500 mV and a broad, multicomponent cathodic peak on the reverse sweep at −500 mV. The anodic peak is assigned to the oxidation of nondiamond carbon impurities at the surface, presumably forming a variety of carbon−oxygen functionalities.[1,24,26,27] The cathodic peak is assigned to the reduction of some of the oxidized surface functionalities and to the reduction of dissolved oxygen generated on the forward sweep. The oxygen evolution current at 2000 mV is very large. After acid washing and rehydrogenation, the voltammetric response changes considerably. The anodic and cathodic peaks associated with the redox reactions involving the nondiamond carbon impurities are absent, consistent with their removal. There is an increase in the overpotential required for oxygen evolution with the current at 2000 mV decreasing by over a factor of 3. There is also an increase in the overpotential for required for hydrogen evolution. This is expected as the treatment removes nondiamond carbon impurities from the surface that have lower overpotential for solvent electrolysis compared to diamond.[24,26] However, the treatment has no effect on the fraction of grain boundaries exposed or other structural defects inherently present in the polycrystalline films. Finally, the diamond surface is not immune to oxidation. In fact, the XPS atomic O/C ratio increases from <0.02 to ∼0.15 after acid washing. The surface termination can also be changed from hydrogen to oxygen at applied potentials as a low as 1.0 V vs SCE in acidic media.[28] However, a big difference between oxidation of diamond and sp^2 carbon electrodes is that the reactions are confined to the surface of the former and do not produce any morphological or microstructural damage due to the strong three-dimensional bonding and high atomic density of the material. It is necessary to mention that removal of the surface nondiamond carbon phases is often not detected by Raman spectroscopy. This is because (i) normally these impurities are at very low levels and are randomly distributed over the surface and (ii) the spectroscopic measurement, unlike the electrochemical one, probes the subsurface as well as the surface microstructure of the films.

Voltammetry at an NRL Film. Panels A−F of Figure 5 show cyclic voltammetric $i-E$ curves for $Fe(CN)_6^{3-/4-}$, $Ru(NH_3)_6^{3+/2+}$ $IrCl_6^{2-/3-}$, dopamine, ascorbic acid, and $Fe^{3+/2+}$, respectively, at a high-quality, free-standing NRL film (No. 148). The electrochemical response of this film was explored because of the recognized high quality of the material. The voltammetric data and apparent electron-transfer rate constants, k^o_{app}, are summarized in Table 1. No correction was made for double-layer or iR effects; therefore,

(27) Swain, G. M. *J. Electrochem. Soc.* **1994**, *141*, 3382.

(28) Hanks, A.; Swain, G. M., unpublished results.

Table 1. Cyclic Voltammetric Data and Apparent Heterogeneous Electron-Transfer Rate Constants for Several Redox Systems at a High-Quality NRL Diamond Thin Film (No. 148)[a].

compound	ΔE_p (mV)	I_p^{ox} (μA/cm^2)	k^o_{app} (cm/s)	α
$Fe(CN)_6^{3-/4-}$	71	305	0.017	0.50
$Ru(NH_3)_6^{3+/2+}$	74	320	0.012	0.50
$IrCl_6$2−/3−	78	330	0.010	0.50
dopamine	480	675	7.3×10^{-5}	0.35
ascorbic acid	E_p^{ox} =781	340		
$Fe^{3+/2+}$	581	140	4.5×10^{-5}	0.65

[a] All redox analyte concentrations were 1 mM. The supporting electrolyte for $Fe(CN)_6^{3-/4-}$, $Ru(NH_3)_6^{2+/3+}$, and $IrCl_6^{2-/3-}$ was 1 M KCl and for dopamine, ascorbic acid, and $Fe^{2+/3+}$ was 1 M $HClO_4$. Data shown are for the fifth scan. Scan rate, 0.1 V/s. k^o_{app} and α-values determined from digital simulations using a commercial software package, DigiSim 1.0 (Bioanalytical Systems, Inc., West Lafayette, IN). Oxidation peak currents normalized to the geometric area of the electrode (0.2 cm^2).

these are only apparent rate constants. The oxidation peak current for each of the analytes varied linearly with (scan rate)$^{1/2}$ from 100 to 500 mV/s ($r^2 > 0.998$) indicative of reaction control by semi-infinite linear diffusion of the reactant to the interface. These redox systems were selected for testing because of known sensitivity or insensitivity of each to the electronic properties, surface microstructure, and surface chemistry of sp^2 and sp^3 carbon electrodes (HOPG, glassy carbon, and diamond).[1,2,10−15] This film was acid washed and rehydrogenated prior to use, meaning that the surface was free of surface nondiamond carbon phases and hydrogen terminated. However, the treated electrode was stored in the open laboratory atmosphere for several months prior to the voltammetric measurements.

$Fe(CN)_6^{3-/4-}$ behaves anomalously on carbon and metal electrodes and does not involve simple electron transfer in which the electrode acts as a source and sink for electrons. There are several factors known to influence the electrode kinetics at metal and sp^2 carbon electrodes. First, the rate of reaction is strongly influenced by the fraction of edge plane exposed on sp^2 carbon electrodes (i.e., electronic properties), but relatively insensitive to the surface oxygen functionalities terminating the edge plane carbon atoms as long as a thick, anionically charged oxide film is not present.[10,11,29,30] The rate of reaction increases proportionally with the fraction of exposed edge plane, as measured by Raman spectroscopy. Second, surface cleanliness is important, as is the electrolyte type and concentration.[10−13,31−33] For example, the involvement of specifically adsorbed cations (e.g., K^+) through a possible surface-bridging interaction has been proposed.[31,32] The rate of reaction increases with electrolyte composition in the order of LiCl < NaCl < KCl.[31−33] At the 1 M electrolyte concentration, the rate is a factor of ~10 higher in KCl than in LiCl at both gold and glassy carbon electrodes.[31,32] Third, adsorbed monolayers on sp^2 carbon electrodes can decrease the rate of reaction. The McCreery group observed an increase in ΔE_p from 5 to 140 mV after modification of the polished glassy carbon surface with adsorbed monolayers.[11,12] The level of increase depends on the type and coverage of the adsorbate.

The electrode kinetics are also influenced by the physicochemical properties of boron-doped diamond. ΔE_p is very sensitive to the surface termination with the smallest ΔE_p observed at the clean, hydrogen-terminated surface. After oxygen termination, ΔE_p increases by over 125 mV but is reversibly reduced to the original value after removal of the oxygen functionalities by hydrogen plasma treatment.[28,34] The sensitivity of the electrode kinetics to surface oxygen at diamond is in sharp contrast to the minor effects these functionalities have on the response at sp^2 carbon electrodes. The rate of reaction is also sensitive to the electrolyte composition and ionic strength with the largest values observed in KCl and the smallest in LiCl. However, the difference at the 1 M concentration level is only a factor of 2−3 rather than 10, as is the case for metal and glassy carbon electrodes.[35] All the evidence at sp^2 carbon and diamond electrodes suggests the involvement of a clean, non-oxide surface site.

ΔE_p for the curve shown is 70 mV (Figure 5A) consistent with k^o_{app} of 0.017 cm/s. This is within 1 order of magnitude of the largest rate constants observed at "activated" glassy carbon surfaces by vacuum heat treatment (0.1 cm/s),[36] ultraclean polishing (0.14 cm/s),[37] and laser activation (>0.5 cm/s).[38] Heterogeneous electron-transfer rate constants at diamond have been reported to range from 10^{-6} to 10^{-2} cm/s.[5,17,35,39,40] The low ΔE_p indicates that this high-quality film possesses the requisite surface structure, chemical composition, and electronic properties to support rapid electron transfer for this particular mechanistically complicated redox system.

$Ru(NH_3)_6^{3+/2+}$ involves simple electron transfer on most electrodes including diamond[1,2,17,24,41] and sp^2 carbon.[10−13,15] The electrode kinetics for $Ru(NH_3)_6^{3+/2+}$ are relatively insensitive to the surface microstructure, surface oxides, and adsorbed monolayers on sp^2 carbon electrodes.[10−12,13,15] The rate of reaction is insensitive to surface modification with the strong implication that electron transfer does not depend on an interaction with a surface site or functional group.[12] The most important factor affecting the rate of reaction is the electronic properties of the electrode, specifically the density of electronic states near the formal potential of the redox system. Of course, with metal and glassy carbon electrodes, a low density of electronic states is seldom an issue. However, with semiconducting/semimetallic diamond, the potential-dependent electronic density of states is an important factor governing the response. This is why ΔE_p increases at diamond with decreasing boron doping level.[41,42]

(29) Chen, Q.; Swain, G. M. *Langmuir* **1998**, *14*, 7017.
(30) Deakin. M. R.; Stutts, K. J.; Wightman, R. M. *J. Electroanal. Chem*. **1986**, *182*, 113.
(31) Bindra, P.; Gerischer, H.; Peter, L. M. *J. Electroanal. Chem. Interfacial Electrochem*. **1974**, *57*, 435.
(32) Peter. L. M.; Dürr, W.; Bindra, P.; Gerischer, H. *J. Electroanal. Chem*. **1976**, *71*, 31.
(33) Noel, M.; Anantharaman, P. N. *Analyst* **1985**, *110*, 1095.
(34) Granger, M. C.; Swain, G. M. *J. Electrochem. Soc.* **1999**, *146*, 4551.
(35) Wang, J.; Swain, G. M. *J. Electroanal. Chem*., submitted.
(36) Fagan, D. T.; Hu, I. F.; Kuwana, T. *Anal. Chem*. **1985**, *57*, 2759.
(37) Hu, I. F.; Karweik, D. H.; Kuwana, T. *J. Electroanal. Chem*. **1985**, *188*, 59.
(38) Rice, R. J.; McCreery, R. L. *Anal. Chem*. **1989**, *61*, 1637.
(39) van de Lagemaat, J.; Vanmaekelbergh, D.; Kelly, J. J. *J. Electroanal. Chem*. **1999**, *475*, 139.
(40) Modestov, A. D.; Pleskov, Y. V.; Varnin, V. P.; Teremetskaya, I. G. *Russian J. Electrochem*. **1997**, *33*, 60.
(41) Vinokur, N.; Miller, B.; Avyigal, Y.; Kalish, R. *J. Electrochem. Soc*. **1996**, *143*, L238.
(42) Lévy-Clément, C.; Zenia, F.; Awa Ndao, N.; Deneuville, A. *New Diamond Frontier Carbon Technol.* **1999**, *9*, 189.

ΔE_p in the curve shown is 74 mV (Figure 5B) consistent with k^o_{app} of 0.012 cm/s. A typical rate constant for ultraclean polished glassy carbon is 0.24 cm/s.[12] ΔE_p is largely unaffected by changing from a hydrogen to an oxygen surface termination.[28,34] The formal potential (i.e., cyclic voltammetric $E_{p/2}$ value) for this couple is −218 mV vs SCE. The valence band position of boron-doped polycrystalline diamond has been estimated to be ∼550 mV vs SCE.[2,5] Considering the 5.4-eV band gap, this means that the formal potential falls within the band gap (i.e., between the valence and conduction band positions). Therefore, this redox system is not expected to exchange charge directly with either the valence or the conduction band. The nearly reversible response indicates that there must be a sufficient density of electronic states present within the band gap at this potential. The midgap density of states in the polycrystalline films can be influenced in a combined way by the boron-doping level and lattice hydrogen content, the inherent grain boundaries and other morphological defects, and the nondiamond carbon impurity phases at the surface. However, in this case, surface nondiamond carbon phases are clearly not an important factor influencing the density of states since the film was acid washed and rehydrogenated. As will be discussed below, the evidence suggests that the boron-doping level and the lattice hydrogen are the most important factors controlling the density of electronic states in this potential region.

$IrCl_6^{2-/3-}$ involves simple electron transfer on most electrodes including diamond[5,34] and sp^2 carbon.[12] The rate of reaction is relatively insensitive to the surface microstructure, surface oxides, and adsorbed monolayers on sp^2 carbon electrodes.[10−13] Surface cleanliness is important, although to a lesser degree than for $Fe(CN)_6^{3-/4-}$. The most influential factor is the electronic structure of the electrode. In the present example, ΔE_p is 78 mV (Figure 5C) consistent with a k^o_{app} of 0.010 cm/s. This is ∼1 order of magnitude lower than the 0.5 cm/s value reported for ultraclean polished glassy carbon.[12] ΔE_p is largely unaffected by changing from a hydrogen to an oxygen surface termination.[34]The formal potential is ∼650 mV vs SCE, which is positive of the proposed valence band position.[5] This means that charge exchange for this couple likely occurs through the valence band and not through midgap states.

Dopamine exhibits much more electrochemical irreversibility, as evidenced by the relatively large ΔE_p. This more irreversible behavior is characteristic of all the catechols and catecholamines investigated so far at diamond.[5,17,24,43] ΔE_p is 480 mV (Figure 5D), consistent with a k^o_{app} of 7.3×10^{-5} cm/s. The rate constant is ∼3 orders of magnitude lower than those for the inorganic redox systems. For comparison, ΔE_p at polished glassy carbon under identical conditions is in the range of 125−175 mV.[29] The formal potential is positive of that for $Fe(CN)_6^{3-/4-}$ so a low density of electronic states is not the reason for the larger ΔE_p. The ΔE_p at diamond is largely unaffected by changing the surface termination from hydrogen to oxygen, leading to the conclusion that surface carbon−oxygen functionalities are not influential.[43] We suppose a lack of adsorption on diamond is one of the reasons for the relatively slow electrode kinetics. Recent work with several catechols and catecholamines has revealed no evidence for adsorption at solution concentrations as low as 1 μM.[44] Indirect support for this supposition also comes from the knowledge that other polar analytes, such as 2,6-anthraquinonedisulfonate, adsorb weakly on diamond at extremely low coverages.[25] Hunt-Duvall and McCreery have presented a detailed study showing that low ΔE_p values correlate with catechol and catecholamine adsorption on glassy carbon, and surface treatments that decreased adsorption also increased ΔE_p.[15]

Ascorbic acid oxidation is chemically irreversible so E_p^{ox} rather than ΔE_p is reflective of the electrode kinetics. This redox reaction has been studied in detail by Hu and Kuwana at glassy carbon,[45] but limited work has been done so far at diamond.[24,43,46] E_p^{ox} at glassy carbon and HOPG shifts negatively with increasing fraction of clean edge plane exposed, but is relatively insensitive to the presence of the oxides terminating the edge plane sites.[10−13,36] The consensus is that ascorbic acid oxidation is catalyzed by a specific, non-oxide surface site.[12,36] E_p^{ox} is very sensitive to the surface termination on diamond shifting positive by 200 mV or more with increasing surface oxide coverage.[28,43] ΔE_p can be returned to the original less positive value after rehydrogenating the surface in a hydrogen plasma.[28] E_p^{ox} in the present case is 791 mV (Figure 5E) and is generally some 200 mV more positive than E_p^{ox} under identical conditions for polished glassy carbon. It may be that the more positive E_p^{ox} at diamond results from a lack of adsorption. Recent coulometric measurements and semi-integral analysis of cyclic voltammetric data have revealed no evidence for adsorption on diamond from solution concentrations as low 1 μM.[28] Considering that E_p^{ox} is positive of the proposed valence band position, it is likely that ascorbic acid exchanges charge directly with this band.

Very sluggish electrode kinetics are observed for $Fe^{3+/2+}$ on diamond, as evidenced by the large ΔE_p of 581 mV (Figure 5F), consistent with k^o_{app} of 4.5×10^{-5} cm/s. This is 2−3 orders of magnitude lower than what is typically observed at polished glassy carbon.[15] The electrode kinetics for $Fe^{3+/2+}$ are highly sensitive to the presence of oxides on sp^2 carbon electrodes. The McCreery group has shown that electron transfer for this system is catalyzed by a specific chemical interaction with surface carbonyl functionalities.[11,12,47] In fact, as the carbonyl coverage increases, the rate of reaction also increases in a near-linear fashion. Removal of the surface oxides by vacuum heat treatment, hydrogen plasma treatment,[29] coverage with nonspecific adsorbers, or site blocking of surface carbonyls inhibits the rate of electron transfer.[11] Therefore, we conclude that the sluggish electrode kinetics at diamond are due to the absence of mediating surface carbon−oxygen functionalities, specifically carbonyl groups. At present, we have not studied this system at oxygen-terminated diamond electrodes so the effect these functional groups might have is unknown.

The voltammetric data presented above reveal that, for $Fe(CN)_6^{3-/4-}$, $Ru(NH_3)_6^{3+/2+}$, and $IrCl_6^{2-/3-}$, the clean, hydrogen-terminated NRL film yields a very active response without any conventional pretreatment prior to use (i.e., mechanical polishing).

(43) Popa, E.; Notsu, H.; Miwa, T.; Tryk, D. A.; Fujishima, A. *Electrochem. Solid-State Lett.* **1999**, *2*, 49.

(44) Chen, Q.; Swain, G. M., unpublished.

(45) Hu, I. F.; Kuwana, T. *Anal. Chem.* **1986**, *58*, 3235.

(46) Chen, Q.; Wang, J.; Swain, G. M.; Sakaguchi, I.; Nishitani-Gamo, M.; Ando, T. unpublished.

(47) McDermott, C. A.; Kneten, K. R.; McCreery, R. L. *J. Electrochem. Soc.* **1993**, *140*, 2593.

Table 2. Cyclic Voltammetric Data and Apparent Heterogeneous Electron Rate Constants for Several Redox Systems at High-Quality USU Diamond Thin Films[a].

redox analyte	ΔE_p (mV)	I_p^{ox} (μA/cm^2)	k^o_{app} (cm/s)	α
$Fe(CN)_6^{3-/4-}$	97 ± 5	960 ± 13	0.019	0.50
$Ru(NH_3)_6^{3+/2+}$	99 ± 6	890 ± 15	0.017	0.50
$IrCl_6^{2-/3-}$	60	117	0.308 ± 0.090	0.50
methyl viologen ($MV^{2+/+}$)	63	400	0.247 ± 0.120	0.50
chlorpromazine ($CPZ^{0/+}$)	99 ± 12	71.0 ± 3.6	0.023	0.50
$Fe^{3+/2+}$	837 ± 42	435 ± 20	1.0×10^{-5}	0.65
dopamine	509 ± 28	1,970 ± 12	3.2×10^{-4}	0.35
4-methylcatechol	471 ± 54	1,995 ± 21	5.3×10^{-4}	0.35

[a] For all redox systems, except $IrCl_6^{2-/3-}$ and $MV^{2+/+}$, the cyclic voltammetric data shown are averages and standard deviations for three films. The concentration of all redox analytes was 1 mM except for chlorpromazine and $IrCl_6^{2-/3-}$, which were both 0.1 mM. The supporting electrolyte for $Fe(CN)_6^{3-/4-}$ and $Ru(NH_3)_6^{+2/+3}$, $IrCl_6^{2-/3-}$, and $MV^{+2/+}$was 1 M KCl, for chlorpromazine was 0.1 M KCl/0.01 M $HClO_4$ and for dopamine, 4-methylcatechol, and $Fe^{2+/3+}$ was 1 M $HClO_4$. Data shown are for the fifth scan. The scan rate for $IrCl_6^{2-/3-}$ and $MV^{2+/+}$ data was 0.1 V/s. All other data were obtained at 1 V/s. k^o_{app} and α-values determined from digital simulations using a commercial software package, DigiSim 1.0 (Bioanalytical Systems, Inc.). k^o_{app} for $IrCl_6^{2-/3-}$ and $MV^{2+/+}$ was also determined according to the theoretical treatment of Nicholson and Shain.[48] Oxidation peak currents normalized to the geometric area of the electrode (0.2 cm^2).

k^o_{app} for each is within a factor of 10 of some of the highest values reported for freshly activated glassy carbon. In the case of $Fe(CN)_6^{3-/4-}$, the hydrogen-terminated surface has the requisite structure for this surface-sensitive reaction. The relatively large k^o_{app}, even though the films were acid washed and rehydrogenated, indicates that nondiamond carbon impurity phases are not an influential factor in the electron transfer, either by direct mediation or by influencing the midgap density of electronic states. The voltammetric data were obtained on free-standing films, so any direct influence of the substrate is eliminated. On the other hand, a relatively low k^o_{app} is observed for $Fe^{3+/2+}$ at hydrogen-terminated diamond, presumably because of the absence of surface carbonyl functional groups. Relatively slow electrode reaction kinetics are also observed for ascorbic acid and dopamine, presumably due to weak adsorption on hydrogen-terminated diamond.[27,48] Further study is required to fully understand the reason for the sluggish kinetics of these redox systems.

Voltammetry at USU Films. Similar voltammetric measurements were made to evaluate and compare the response of our high-quality films with the high-quality NRL film. The results for $Fe(CN)_6^{3-/4-}$, $Ru(NH_3)_6^{3+/2+}$, $IrCl_6^{2-/3-}$, dopamine, and $Fe^{3+/2+}$ are presented along with additional data for methyl viologen, chlorpromazine, and 4-methylcatechol. Table 2 summarizes the cyclic voltammetric data and k^o_{app} values for these redox systems at acid-washed and rehydrogenated films. For all the redox systems except $IrCl_6^{2-/3-}$ and $MV^{+2/+}$, the data shown are the average and standard deviations for three films at a scan rate of 1 V/s. The data for these two systems are for one electrode at a scan rate of 0.1 V/s. k^o_{app} for all except $IrCl_6^{2-/3-}$ and $MV^{+2/+}$ was estimated from the data at 1 V/s. k^o_{app} shown for $IrCl_6^{2-/3-}$ and $MV^{+2/+}$ is the average and standard deviation for measurements made at scan rates from 0.1 to 0.5 V/s. It can be seen that similar results are obtained with our high-quality films as compared to the high-quality NRL film. The oxidation peak current for each of the analytes varied linearly with the square root of the scan rate ($r^2 > 0.998$) from 100 to 500 mV/s and linearly with the concentration ($r^2 > 0.998$) from 1 mM to 1 μM. Both plots had near-origin *y*-axis intercepts. Good reproducibility was observed for the films, based on the variability in ΔE_p values. Variability of ~5% is seen for $Fe(CN)_6^{3-/4-}$, $Ru(NH_3)_6^{+2/+3}$, $Fe^{2+/3+}$, and dopamine, while a larger variation of ~11% is seen for chlorpromazine and 4-methylcatechol. k^o_{app} for $Fe(CN)_6^{3-/4-}$, $Ru(NH_3)_6^{3+/3+}$, and $IrCl_6^{2-/3-}$ is 0.019, 0.017, and 0.308 ± 0.09, respectively. Again, k^o_{app} for $IrCl_6^{2-/3-}$ was determined at scan rates from 0.1 to 0.5 V/s according to the theory developed by Nicholson and Shain.[48] k^o_{app} for $Fe(CN)_6^{3-/4-}$ and $Ru(NH_3)_6^{2+/3+}$ at both the USU and NRL films is nearly the same. The big difference between the two films is k^o_{app} for $IrCl_6^{2-/3-}$,which is 1 order of magnitude larger at the USU film, and is close to the highest value reported for freshly activated glassy carbon.[12]

k^o_{app} for methyl viologen ($MV^{2+/+}$) is 0.247 and is slightly higher than the 0.094 ± 0.025 cm/s reported for polished glassy carbon.[14] This redox system involves simple electron transfer at diamond[5,17,24,34,41,46] and most other electrodes.[14] The rate of reaction at diamond is relatively insensitive to surface oxides, grain boundaries, and defect density and the presence of nondiamond carbon impurities.[5,17,24,34,46] Like $Ru(NH_3)_6^{3+/2+}$, the most important factor influencing the rate is the density of electronic states at the formal potential. The formal potential of ~−700 mV vs SCE is well into the band gap region, even more negative than the formal potential for $Ru(NH_3)_6^{3+/2+}$. Therefore, methyl viologen likely undergoes charge transfer through midgap surface states. The large k^o_{app} indicates that a sufficient midgap density of electronic states exists at even these negative potentials.

Results for the chlorpromazine ($CPZ^{+/0}$), formerly used as an antipsychotic drug to treat psychosis and other mental ailments, are also presented. Voltammetric studies of this analyte have been reported at both freshly activated glassy carbon[14] and diamond.[24] The results obtained so far indicate that the rate of electron transfer at diamond is insensitive to the surface microstructure and chemistry.[24] k^o_{app} is 0.023 cm/s and is similar to the rate constant reported for other diamond films[24] and polished glassy carbon.[14] The formal potential is ~650 mV vs SCE. Therefore, charge exchange is expected to occur directly with the valence band.

Sluggish electrode kinetics are observed for dopamine, 4-methylcatechol, and $Fe^{3+/2+}$, consistent with the results for the high-quality NRL film. k^o_{app} is 3.2×10^{-4}, 5.3×10^{-4}, and 1.0×10^{-5} cm/s, respectively. The rate constant for dopamine is a factor of 2 larger while the rate constant for $Fe^{3+/2+}$ is a factor of 4 lower at the NRL film. The causes for these differences remain unclear at this point. The general finding is still that these redox systems have k^o_{app} several orders of magnitude lower than the inorganic ($Fe(CN)_6^{3-/4-}$, $Ru(NH_3)_6^{3+/2+}$, and $IrCl_6^{2-/3-}$) and organic redox systems ($MV^{2+/+}$ and $CPZ^{+/0}$).

Model for Electron Transfer at Boron-Doped Polycrystalline Diamond. Diamond is a wide band gap semiconductor (~5.4 eV), and the interfacial energetics of the semiconductor−electrolyte interface are governed by the spatial dependence of

(48) Nicholson, R. S.; Shain, I. *Anal. Chem.* **1964**, *36*, 706. Nicholson, R. S. *Anal. Chem.* **1965**, *37*, 1351.

the potential drop at the interface and the relative positions of the energy levels within the semiconductor bulk, surface states, and solution species.[39,49−51] A discussion of electron transfer at diamond requires a model to explain the thermodynamic and kinetic aspects of the reactions. The well-accepted Gerischer model has been used to explain electron transfer at semiconductor electrodes. According to this theory,[50] electron transfer at an ideally behaved semiconductor electrode is proportional to the potential-dependent density of occupied (cathodic or reduction current) and unoccupied (anodic or oxidation current) electronic states at the formal potential of the redox analyte. The energy levels of the charge carriers and their absolute density at a particular energy (i.e., potential) define the density of states of a material. Ideally for wide band gap semiconductors such as diamond, current flow will be dominated by the band closest in energy to the formal potential of the redox couple, at least at equilibrium.[50] Equilibrium between a semiconductor electrode and a redox system can result in a situation where the Fermi level is located in the band gap of the semiconductor. In such situations, the current flow is inhibited because of a limited number of charge carriers (holes and electrons). However, due to the gross inhomogeneities associated with the bulk and interface of polycrystalline materials, it is extremely difficult to apply this idealized model of electron transfer to such materials in a quantitative way.[51]

Boron-doped, polycrystalline diamond electrodes deviate from ideal *p-type* semiconductor behavior because of a high density of midgap electronic states. The midgap density of states results from at least four factors: (i) boron-doping level, (ii) lattice hydrogen content, (iii) inherent grain boundaries and other defects in the polycrystalline films, and (iv) nondiamond carbon impurity phases at the surface. Of these four factors, it is clear that surface nondiamond carbon impurities are not influencing the response of these films due to the acid washing and hydrogen plasma treatment. The role of the other three factors are discussed below.

The boron-doping level and uniformity are important factors governing the electrode kinetics. For example, a correlation between the doping level and ΔE_p for $Ru(NH_3)_6^{3+/2+}$ has been reported in the literature.[41,42] As boron is added to the lattice, electrical conduction takes place through hopping, and at very high doping levels ($N_a > 10^{19}$ B/cm^3), impurity band conduction occurs. Boron is easily incorporated into substitutional sites within the diamond lattice without causing lattice distortion.[52] Nishimura et al. reported that in heavily boron doped films ($N_a \sim 10^{20}$ B/cm^3) an impurity band is likely formed. At high doping levels, the overlapping wave functions of nearby acceptor centers leads to band formation. Metallic conduction in heavily boron-doped ($N_a \sim 10^{21}$ B/cm^3), polycrystalline films was reported.[53] The activation energy decreased with doping density as impurity band conduction dominated, and at sufficiently high concentrations, the impurity band merged with the valence band leading to metallic conduction. The activation energy of a boron acceptor is near 0.37 eV.[52] For highly doped films, activation energies as low as 0.002 eV have been reported due to band formation.[52]

The role of morphological defects and grain boundaries on the electrode kinetics, specifically the electrical conduction, at polycrystalline films is still not clearly understood. Diamond is host for a variety of extended defects such as stacking faults, microtwins, dislocations, nondiamond carbon phases, grain boundaries, and mixed habit growth features. These defects could serve as discrete sites for electron transfer or could simply affect the electronic properties of the material by increasing the density of states. Undoped polycrystalline films have some inherent electrical conduction, presumably because of the density of states arising from the grain boundaries and other defects. The grain boundaries could contain nondiamond carbon impurity phases giving rise to additional midgap surface states and reactive sites. On the other hand, the electrical conduction could be inhibited by grain boundaries and defects because of a reduction in the electron and hole mobilities. We are attempting to understand the relative influence of grain boundaries and other defects on the electrochemical response by using a low-defect, diamond (100) electrode.[46] Preliminary voltammetric measurements were made at a boron-doped (1×10^{19} B/cm^3) diamond thin film (1.5-μm estimated thickness) that was homoepitaxially deposited on a (100) oriented HPHT substrate. $Fe(CN)_6^{3-/4-}$, $Ru(NH_3)_6^{3+/2+}$, methyl viologen ($MV^{2+/+}$ and $MV^{+/0}$), and 4-*tert*-butylcatechol were used to probe the electrode response. The cyclic voltammetric ΔE_p values (*iR* uncorrected) at 0.05 V/s were 210, 75, 85 and 90, and 850 mV, respectively, for the redox systems. The most important observation related to the present discussion is the relatively small ΔE_p for $Ru(NH_3)_6^{3+/2+}$ and for both couples of methyl viologen ($MV^{2+/+}$ and $MV^{+/0}$). Both of these redox systems have formal potentials well into the band gap region and yet the relatively low ΔE_p values indicate a sufficient density of states exist at these potentials for relatively rapid electron transfer. The fact that these ΔE_p are so low even though this surface has negligible defects, at least compared to the polycrystalline films, suggests that defects and grain boundaries do not contribute significantly to the midgap density of electronic states for films doped in the low 10^{19} B/cm^3 range or greater. These preliminary results indicate that the midgap density of states arising from grain boundaries and defects is relatively low compared to the number arising from the boron doping and lattice hydrogen. Further work is currently in progress using both diamond (100) and (111) electrodes to better understand the role of defects and grain boundaries on the electrochemical response.

Hydrogen incorporated in diamond, like boron, plays an important role in the electrode kinetics.[52] Hydrogen incorporation gives diamond *p-type* semiconductor electronic properties. The electrical properties of diamond strongly depend on the concentration of this impurity. For example, when subsurface hydrogen is present an increased electrical conductivity is observed because of increased hole conduction, hence the *p*-type character of the surface region of diamond. Hydrogen exists in both bonded and nonbonded configurations. The important role of bonded surface hydrogen on k^o_{app} for some redox systems has already been discussed. The importance of nonbonded hydrogen on the carrier transport rates in boron-doped diamond has been reported.[54]

(49) Boonma, L.; Yano, T.; Tryk, D. A.; Hashimoto, K.; Fujishima, A. *J. Electrochem. Soc.* **1997**, *144*, L142.
(50) Gerischer, H. *Electrochim. Acta* **1990**, *35*, 1677.
(51) Koval, C. A.; Howard, J. N. *Chem. Rev.* **1992**, *92*, 411.
(52) Zhu, W. In *Diamond: Electronic Properties and Applications*; Pan, L. S., Kania, D. R., Eds.; Kluwer Academic Publishers: Boston, 1995; Chapter 5 and references therein.
(53) Nishimura, K.; Das, K.; Glass, J. T. *J. Appl. Phys.* **1991**, *69*, 3142.

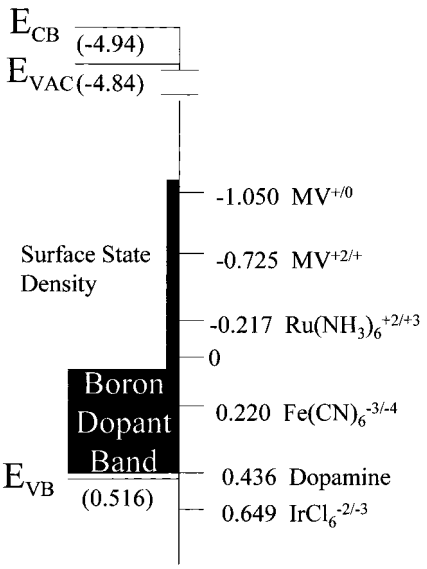

Figure 6. Proposed energy diagram for the diamond−electrolyte interface.

Researchers have found that an electrically resistive diamond film surface becomes much more conducting after annealing in atomic hydrogen.[55−58] Looi et al. determined that hydrogen promotes the formation of gap states in polycrystalline diamond, some of which act as shallow acceptors. Heating the samples either in air or in vacuo results in increased electrical resistivity due to a loss of near-surface, nonbonded rather than chemisorbed hydrogen. The unbonded hydrogen in the lattice desorbs at temperatures less than 400 °C while the bonded hydrogen does not desorb at any significant rate until 1000 °C.[57] Hayashi and co-workers have used SIMS to characterize the depth of the hydrogenated region and found it to penetrate ∼20 nm into the sample.[54] Interestingly, this subsurface hydrogen is absent in films exposed to oxidizing conditions.

Figure 6 shows a proposed interfacial energy diagram for a high-quality, hydrogen-terminated, polycrystalline diamond electrode, boron doped at a level of 1×10^{19} B/cm^3 or greater. The formal potentials of several redox systems (as determined from the cyclic voltammetric $E_{p/2}$ values) are shown relative to the proposed band edge positions. Determining the band positions requires a knowledge of the flat-band potential. Most of the reported flat-band potentials range from 450 to 1000 mV vs SCE.[2,5,49,59] The band positions shown were reported in a previous publication and were determined using a flat-band potential of 455 mV vs SCE and a band gap of 5.4 eV.[5] The interfacial energy diagram shows that the midgap density of electronic states is controlled primarily by two factors: the boron-doping level and surface states arising from lattice hydrogen. For reasons discussed already, nondiamond carbon impurity phases, grain boundaries, and other defects are less influential. What we do not know is how far into the band gap the boron dopant band or the hydrogen surface state density extend. What is for sure is that a sufficient density of midgap electronic states exists to ∼−1100 mV vs SCE to support rapid electron transfer at redox analyte concentrations of 1 mM or less. What is not known is how these states are distributed between the boron dopant and lattice hydrogen levels. In previous work, we proposed an interfacial energy diagram for the diamond−electrolyte interface in which the midgap states were presumed to result from nondiamond carbon impurity phases.[5] We now know that nondiamond carbon phases exert little influence, both directly or indirectly, on the electrochemical response of high-quality, boron-doped diamond films.

CONCLUSIONS

The electrochemical response of high-quality, boron-doped diamond thin films from two different sources was compared: a community-recognized high-quality film from NRL and high-quality films from our group. Some of the factors that influence the electrode kinetics for several aqueous-based redox systems were investigated, in particular, the role of nondiamond carbon surface impurity phases. The similarity of the voltammetric data for the NRL and USU films indicates the high quality of the latter. In our opinion, these data can serve as an all-important benchmark for diamond electrode performance. Several important conclusions regarding the structure−reactivity relationship at diamond electrodes can be made. First, $Ru(NH_3)_6^{3+/2+}$, $IrCl_6^{2-/3-}$, methyl viologen, and chlorpromazine exhibit k^o_{app} in the low to 10^{-2}−10^{-1} cm/s range and appear to involve simple electron transfer that is relatively insensitive to surface oxides, to grain boundaries and other defects present in the polycrystalline films, and to nondiamond carbon impurities. The main factor influencing k^o_{app} is the density of electronic states at the formal potential of the redox couple. k^o_{app} $Ru(NH_3)_6^{3+/2+}$ and methyl viologen have formal potentials that fall well into the midgap region of diamond. The large k^o_{app} for both suggests a sufficient density of electronic states exists near the formal potentials (approximately −200 and −700/−1050 mV vs SCE, respectively) of each. These midgap states result mainly from the boron doping and the lattice hydrogen rather than from nondiamond carbon impurity phases or grain boundaries and other defects. Second, $Fe(CN)_6^{3-/4-}$ and ascorbic acid involve more complex, surface-sensitive electron transfer with rates (i.e., ΔE_p and E_p^{ox}, respectively) that are highly sensitive to the presence of surface oxides but insensitive to nondiamond carbon impurity phases. The fastest kinetics for both were observed at the hydrogen-terminated surface. The ΔE_p for $Fe(CN)_6^{3-/4-}$ increases and the E_p^{ox} for ascorbic acid shifts positive with increasing oxide coverage. The inhibitory effects of surface oxygen can be removed by rehydrogenating the surface in a hydrogen plasma. k^o_{app} in the low to mid 10^{-2} cm/s range is observed for $Fe(CN)_6^{3-/4-}$ at hydrogen-terminated diamond. These two redox systems appear to be catalyzed by a specific non-oxide surface site. Third, $Fe^{3+/2+}$ undergoes sluggish electron transfer at hydrogen-terminated diamond. Similarly sluggish electron transfer is observed on low-oxide glassy carbon, but the redox reaction can be catalyzed by an inner-sphere pathway at the oxidized surface through carbonyl functionalities. Low k^o_{app} values in the 10^{-5} cm/s range are typical for diamond and result because the inner-sphere pathway is inaccessible due to the absence of carbonyl surface functionalities on the hydrogen-terminated

(54) Hayashi, K.; Yamanaka, S.; Okushi, H.; Kajimura, K. *Appl. Phys. Lett.* **1996**, *68*, 376.
(55) Landstrass, M. I.; Ravi, K. V. *Appl. Phys. Lett.* **1989**, *55*, 975.
(56) Landstrass, M. I.; Ravi, K. V. *Appl. Phys. Lett.* **1989**, *55*, 1391.
(57) Looi, H. J.; Jackman, R. B.; Foord, J. S. *Appl. Phys. Lett.* **1998**, *72*, 353.
(58) Looi, H. J.; Pang, L. Y. S.; Molloy, A. B.; Jones, F.; Foord, J. S.; Jackman, R. B. *Diamond Relat. Mater.* **1998**, *7*, 550.
(59) Sakharova, A. Y.; Pleskov, Y. V.; Di Quarto, F.; Piazza, S.; Sunseri, C.; Teremetskaya, I. G.; Varnin, V. P. *J. Electrochem. Soc.* **1995**, *142*, 2704.

surface. Little work has been performed to date with this system at oxygen-terminated diamond to know how oxides affect the rate constant. Fourth, k^{o}_{app} for dopamine, 4-methylcatechol, and 4-*tert*-butylcatechol is insensitive to the surface termination, grain boundaries and defects, and nondiamond carbon impurity phases. k^{o}_{app} in the $10^{-4}-10^{-5}$ cm/s range is typical. The relatively low rate constants may be related to a lack of adsorption. The slow electrode reaction kinetics for ascorbic acid (E_p^{ox} ~200 mV more positive than the value typically observed at polished glassy carbon) may also be due a lack of adsorption.

ACKNOWLEDGMENT

The research was supported by grants from DOE—Office of Science (DE-FG03-95ER14577), NSF (CHE-9505683), and the donors to the Petroleum Research Fund, administered by the American Chemical Society. We thank Professor Richard McCreery and his group for many helpful discussions.

Received for review January 19, 2000. Accepted June 9, 2000.

AC0000675